Macromolecules

ARTICLE

pubs.acs.org/Macromolecules

Radical Copolymerization of Isobutylene and Ethyl Acrylate with $LiCB_{11}Me_{12}$ Catalyst

Hua Mei,[†,∥] Christos Douvris,[†] Victoria Volkis,[†,⊥] Phillip Hanefeld,[‡] Nicole Hildebrandt,[§] and Josef Michl*[,†]

[†]Department of Chemistry and Biochemistry, University of Colorado, Boulder, Colorado 80309-0215, United States

[‡]BASF Future Business GmbH 4, Gartenweg Z 25, 67063 Ludwigshafen, Germany

[§]BASF SE, GKS/M - B001, 67056 Ludwigshafen, Germany

Supporting Information

ABSTRACT: In nonpolar media $LiCB_{11}Me_{12}$ catalyzes the radical copolymerization of ethyl acrylate with isobutylene. The reaction is initiated by azo-*tert*-butane at 75−80 °C or with UV-irradiated di-*tert*-butyl peroxide at room temperature. Nonalternating copolymers with novel somewhat branched structures were produced and characterized by NMR. Isobutylene incorporation (up to 56 mol %) depends on the comonomer ratio, and a copolymerization mechanism is proposed.

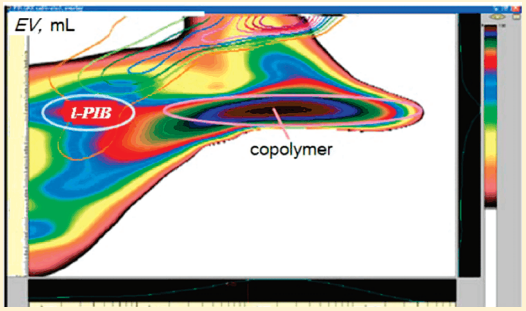

INTRODUCTION

The radical homopolymerization of isobutylene (IB) is unusual but can be accomplished under catalysis with $LiCB_{11}(CH_3)_{12}$ (**1**) in poorly coordinating solvents at ambient pressure and temperature.[1−3] It yields a novel highly branched form of polyisobutylene (*b*-PIB) with molecular weights in the thousands (up to ∼2.5×10^4) according to GPC relative to polystyrene standards. Presently we examine the use of the $LiCB_{11}(CH_3)_{12}$ catalyst with azo-*tert*-butane (ATB) radical initiator for the copolymerization of IB with ethyl acrylate (EA), as previously briefly mentioned in a short communication.[2] We find that it leads to an unusual somewhat branched nonalternating high molecular weight copolymer with up to ∼56 mol % of IB.

EA and IB can be copolymerized, but it is difficult due to different reactivity.[4] IB is normally polymerized cationically to a linear polymer with $AlCl_3$ in halogenated hydrocarbons in the presence of traces of water.[5] In contrast, ethyl acrylate is ordinarily polymerized under radical initiation, sometimes under catalysis with rare earth metal complexes[6] or other metal-containing species.[7−10]

The poor copolymerization potential of IB with acrylic esters in a radical process is apparent from the monomer reactivity ratio. The Alfrey−Price $Q-e$ value[11] reactivity ratio of IB is more than 10 times lower than that of EA.[12] Still, conventional radical copolymerization of the two monomers results in a poly(ethyl acrylate) (PEA) containing a fair number of IB units.[13,14] For example, thermal or UV peroxide initiated radical copolymerization of IB and EA provides a low molecular weight product containing 20−30 mol % of IB.[14] The situation is improved by addition of strong Lewis acids, such as AlR_nCl_{3-n},[15−17] BF_3,[18] $SnCl_4$,[18] $ZnCl_2$,[18] etc. A high molecular weight alternating copolymer containing 50 mol % of IB was obtained using alkylaluminum and alkylboron halides as catalysts.[19]

Metal-catalyzed coordination polymerizations are highly effective for olefins, but less so for polar acrylic monomers. Although recently, functionality tolerant late transition metal catalysts were used to catalyze the copolymerization,[20,21] EA/IB copolymers are still produced commercially by free-radical polymerization because other methods are too costly.[22]

EXPERIMENTAL SECTION

Materials. IB (Airgas) was pure grade (>99%) and was dried over activated 3 Å molecular sieves. EA (Aldrich) was distilled, dried over 4 Å molecular sieves, and stored in a Schlenk tube. 1,2-Dichloroethane (DCE, Aldrich) was dried with P_2O_5 and distilled twice before use. ATB (Aldrich) was ∼97% pure. EA-d_5 and IB-d_8 were ordered from CDN Isotopes Inc. $LiCB_{11}Me_{12}$[23] was dried under reduced pressure (∼0.04 mbar) at 100 °C overnight before use. It contained residual sulfolane in a molar ratio sulfolane:$LiCB_{11}Me_{12}$ = ∼1:10.

Polymerization. Polymerization was conducted in a 25 mL stainless steel pressure reactor with a Teflon insert, a stir bar, and an accurate pressure gauge. In a typical reaction, the dried catalyst (0.1 mmol), DCE (0.50 mL), ATB (0.07 mL), and EA (1.4 mmol) were added to the reactor under argon flow. The reactor was closed, cooled down with liquid nitrogen, and evacuated on a vacuum line. IB (30 mmol) was introduced into the closed system, and the solution was stirred at 75−80 °C for 24 h. After this time, the reactor was allowed to reach room temperature and opened, and

Received: August 20, 2010
Revised: February 9, 2011
Published: March 25, 2011

Table 1. $LiCB_{11}Me_{12}$-Catalyzed ATB-Initiated IB/EA Copolymerization[a]

entry	EA, mmol	EA, mg	cat., mmol	IB, mmol	$M_w/10^4$ [b]	MWD[b]	T_d, °C	EA/IB molar ratio in copolymer[c]	wt % EA in copolymer[c]	copolymer,[d] mg
1	0.92	92	0.10	35.5	5.6	3.2	425	0.7	54	42
2	0.92	92	0.10	165.4	5.3	4.6	275	0.4	44	46
3	0.92	92	0.20	34.2	4.4	1.1	345	0.6	50	91
4	1.84	184	0.10	53.4	4.3	1.1	250	1.7	75	50
5	0.92	92	0.20	137.1	3.6	2.6	432	0.7	54	42
6	0.92	92	0.20	22.3	3.9	4.7	345	0.9	62	105
7	0.92	92	0.20	115.8	3.6	2.1	358	0.8	54	95
8[e]	0.92	92	0.20	22.3	4.4	3.9	376	0.9	57	110
9[f]	0.92	92	0.20	22.3	3.1	4.8		0.9	55	110

[a] Reaction mixture: 0.5 mL of DCE; 10 wt % of radical initiator; thermally initiated (75−80 °C). [b] From GPC with polystyrene standards. [c] Determined by NMR integration. [d] Determined gravimetrically. [e] Similar to run 1, but with IB-d_8 and twice the amount of catalyst. [f] Similar to run 1, but with EA-d_5 and twice the amount of catalyst.

the reaction mixture was quenched with methanol (10 mL). All contents were transferred to a flask, the reactor was rinsed with methanol (10 mL) and THF (10 mL), and the washings were added to the flask. A small amount of solid polymer was removed by filtration and was not investigated further. All the volatiles were removed from the filtrate, first on a rotary evaporator and then under high vacuum. The polymer was extracted from the residue with 50 mL of hexane:THF (80:20). The insoluble part was mostly the catalyst which was regenerated.[2] Hexanes and THF were removed from the soluble part, and the residue was dried overnight in a vacuum line at 120 °C. The sample was dissolved in $CDCl_3$ for the measurement of NMR spectra, evaporated to dryness, and dissolved in THF for GPC analysis. The polymer was dried in an oven at 80 °C at ~0.04 mbar overnight before characterization by thermogravimetry (TGA) and differential scanning calorimetry (DSC).

Measurements. All manipulations were carried out using standard vacuum and inert atmosphere techniques. NMR spectra were taken with 400 and 500 MHz NMR spectrometers at room temperature in $CDCl_3$ unless noted otherwise. Chemical shifts are given in ppm with positive shifts downfield. ^1H chemical shifts were referenced to residual protons from the solvent. Molecular weights and polydispersities of the polymers were determined in THF solutions by the relative GPC method (GPC at ambient temperature, calibrated against Aldrich polystyrene standards). A Waters gel permeation chromatograph, refractive index detector (RI 2414), and EMPOWER software were used, with a three-column bed (Styragel HR 4.6 300 mm columns for molecular weight ranges 100−10 000, 500−30 000, and 5000−6 000 000 and a flow rate of 0.3 mL/min). Representative samples were later analyzed in THF using a GPC system with triple detection (refractive index, RI, right angle light scattering, LS, and intrinsic viscosity, IV) using Viscotek GPC instrument equipped with Viscotek G4000 and G6000 columns and OmniSec Software. TGA and DSC were obtained under nitrogen with a TGA Q500 and DSC Q500 (TA Instruments−Waters LLC), respectively, with heating rates of 10 °C/min. Sample size for TGA was normally 10−20 mg and for DSC, 5 mg. HPLC measurements for copolymers were done using a system equipped with UV-Photometer Agilent 1200 VWD SL, Varian ELSD 2100 [UV = 260 nm] detectors, and a C18, 5 cm, 0.46 mm diameter column. Measurements were performed at 80 °C with a flow rate of 3 mL/min, using a gradient water: THF from 95:5 to 0:100. Two-dimensional HPLC−GPC measurements used (i) in the first dimension, a Waters XBridge C18 50 × 4.6 mm column at 30 °C with a flow rate of 0.05 mL/min, using a gradient water:THF from 95:5 to 0:100, and (ii) in the second dimension, a PSS PFG linM HS 50 × 4.6 mm column at 30 °C with a THF flow rate of 10 mL/min and an ERC Corona detector.

RESULTS

Synthesis and GPC. Table 1 shows the results from nine runs selected from several dozen in which IB and EA were copolymerized at 75−80 °C under various experimental conditions.

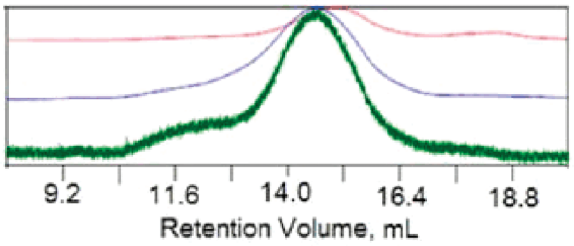

Figure 1. Triple detection GPC of typical copolymer (red, refractive index; green, right angle light scattering; blue, viscometer).

Duplicate experiments gave similar but not exactly identical results, nearly independent of the initial concentration of the monomers. A decrease in the weight ratio of starting comonomers EA/IB increased the degree of incorporation of IB into the copolymer until a ratio of ~1:50 was reached. Beyond this comonomer ratio, no further increase was observed. At 65 °C, little polymer was formed. When the amount of catalyst was increased, the polymer yield increased considerably.

In addition to thermal polymerization, we also performed several runs in which copolymerization was induced at room temperature by UV irradiation in a Pyrex vessel and observed similar results. In these experiments, the pressure of IB was periodically brought up to 1 bar, and its total amount was not known accurately.

Triple-Detection GPC and HPLC Analysis. The copolymers from several runs were also analyzed using a GPC instrument with triple detection, and all yielded similar results. The copolymer is bimodal (Figure 1). For the major component M_w = ~48 000, M_z = ~7600, and M_w/M_n = 2.29. The intrinsic viscosity (IV) is 0.169, and the Mark−Houwink slope is 0.213. The dependence of log R_h (hydrodynamic radius) on log M_w is almost linear. For the minor component M_w = ~136 000, M_z = ~287 000, and M_w/M_n = 2.11, but its RI signal is weak compared to IV and LS signals. The copolymer has a hydrodynamic radius R_h ~ 0.8.

Figure 2 shows the 2D HPLC−GPC of a crude copolymer (filled level curve, a run similar to run 2 in Table 1) and of a mixture of *l*-PIB standards of different M_w (plain, unfilled level curves). It is seen that the crude product consists of two fractions. The small one corresponds to pure *l*-PIB of low molecular weight, and the main one, located underneath the spot for pure *l*-PIB standards, is attributed to the copolymer.

NMR Analysis. ^1H DOSY NMR[24] confirms that the product (Figure 3) contains a copolymer, small traces of organic impurities in some runs, and no detectable homopolymers in most runs. In the

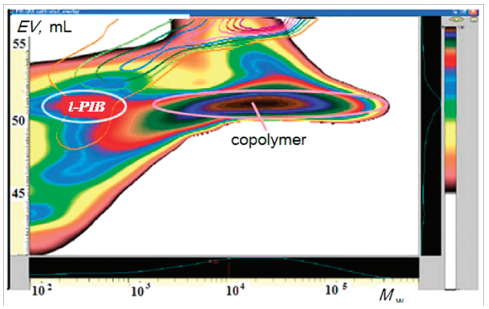

Figure 2. 2D HPLC-GPC of typical copolymer (filled level lines). Superimposed (plain level lines) are results for a mixture of *l*-PIB samples with different M_w.

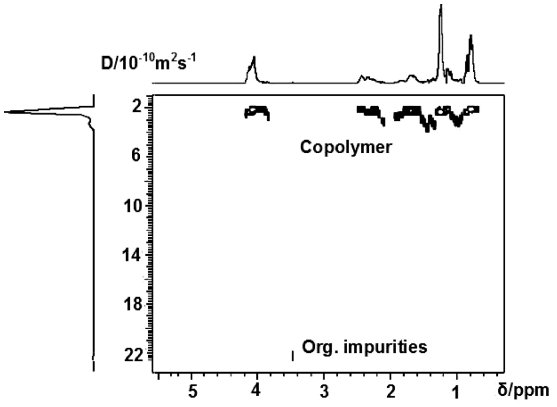

Figure 3. ^{1}H DOSY NMR of typical copolymer.

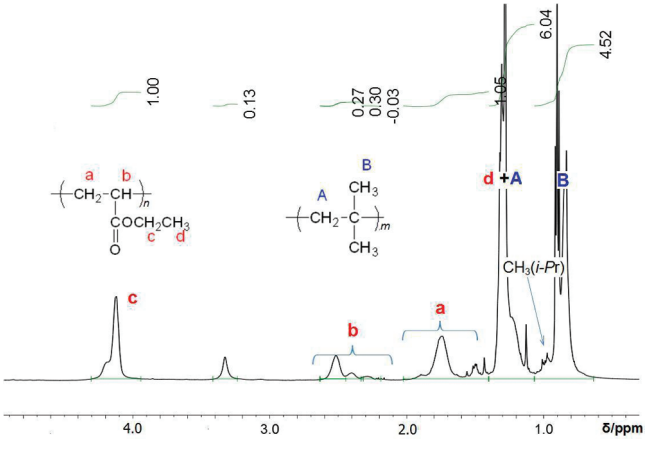

Figure 4. ^{1}H NMR of typical copolymer (see also structures in Figure 5).

copolymers, signals due to the EA part and those due to the IB part of the structure line up at the same value of diffusion coefficient *D*. The intense cross-signal (Figure 3) occurs at $D = \sim 2 \times 10^{-10}$ m^2 s^{-1}, and its ^{1}H NMR corresponds to the copolymer. Under our polymerization conditions, *b*-PIB typically appears at $D = \sim(10-14) \times 10^{-10}$ m^2 s^{-1}, *l*-PIB appears at $D = \sim(6-8) \times 10^{-10}$ m^2 s^{-1}, and PEA appears at $D = \sim 0.5 \times 10^{-10}$ m^2 s^{-1} and below, and their spectra are characteristic and different from the spectrum of the copolymer.

The structure of the copolymers was analyzed by ^{1}H (Figure 4) and ^{13}C (Figure 5) NMR spectroscopy. The EA/IB ratios were determined from ^{1}H NMR integration. The spectra

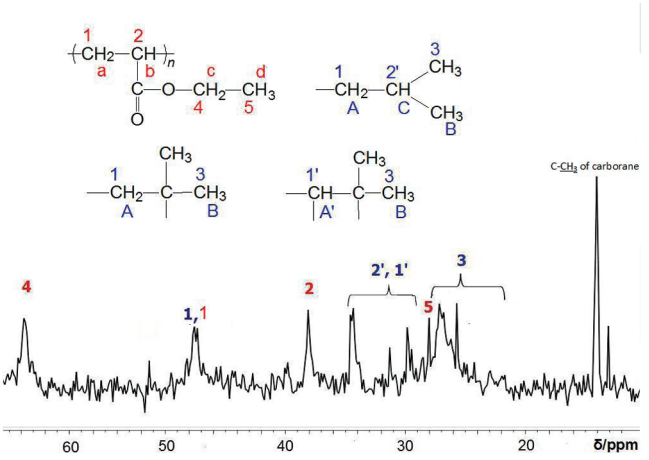

Figure 5. ^{13}C NMR spectrum of typical copolymer with tentative assignment.

do not reveal the presence of any long *l*-PIB fragments in the copolymer but are compatible with *b*-PIB and PEA fragments. Comparison with the known spectra of pure homopolymers *b*-PIB[20] and EA[25] and the results of 2D NMR analysis described below permitted an assignment of the ester (c and d), methylene (a), and methine (b) protons in the EA units to signals at 4.1, 1.3, 1.7, and 2.5 ppm, respectively, and the assignment of the methyl (B) plus methylene (A) protons in the IB units to signals at 0.8−1.0 and 1.3 ppm, respectively (Figure 4). ^{13}C NMR spectra were assigned in a similar manner (Figure 5). The backbone methylene peak 1 is found between 47 and 48 ppm. The backbone methine signal 1′ appears at 29−34 ppm, close to methyl carbons from isobutyl groups and backbone $C(CH_3)_2$ groups. The signal at 38 ppm is assigned to the methine 2. The methylene group 1 of the IB backbone appears at 48 ppm. The methyl group 5 and methylene group 4 of the ethoxy group from EA are assigned at 28 and 64 ppm, respectively. The signals of these carbons are deshielded due to their closeness to oxygen.

The use of gCOSY (Figure 6), gHMBC NMR (Figure 7), and gHSQC (Figure 8) leads to the assignments marked in Figures 4 and 5. In units originating in EA, gCOSY NMR has identified a−b and c−d proton correlations for CH_2-CH segments in the backbone and $-C_2H_5$ groups in the ester. In units originating in IB, the B−C correlation is due to the PIB branch terminating isobutyl group. gHMBC NMR (Figure 7), which uses interaction based on J_2 and longer range coupling, was used to assign links between EA and IB components in the copolymer. Phase-resolved gHSQC NMR (Figure 8) permitted a discrimination between CH_2, on the one hand, and CH_3 or CH groups, on the other hand, and was used to confirm all the assignments.

The 2D NMR results are summarized in Table 2.

Two deuterium-labeled copolymers (entries 8 and 9 in Table 1) were also prepared and analyzed. A copolymer formed from EA and IB-d_8 showed only one broad signal in ^{2}H NMR (Supporting Information). In ^{1}H NMR the intensities of signals of all PIB segments of the deuteriated copolymer were smaller than those in the unlabeled copolymer (Table 1). ^{2}H NMR of the copolymer formed from EA-d_5 and IB showed CD_2 and CD_3 groups in the EA part (Figure 9). Their integrated intensities were in a 1:4−1:5 ratio instead of the anticipated 2:3. Given the poor signal-to-noise level that we were able to achieve, it was not clear whether the difference is significant. It was also unclear whether the additional small peak that

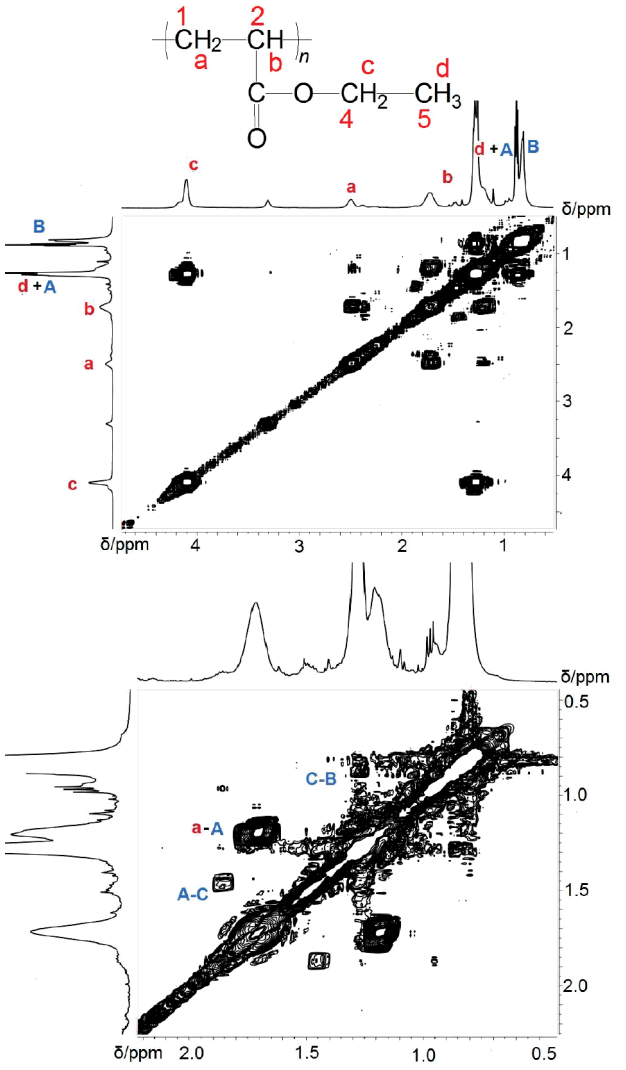

Figure 6. COSY NMR spectrum of typical copolymer with tentative assignments (A: the whole spectrum; B: an expanded section).

appeared in the spectrum is real. Tentatively, we assigned it to a deuteriated isopropyl group.

An attempt to detect the presence of a hydrolyzable ester group in the backbone by hydrolysis and GPC provided little or no evidence for a substantial reduction of the copolymer molecular weight.

Most of the copolymers had glass transition temperatures (T_g) that varied fairly erratically within a narrow range of −18 and −10 °C. In Table 3, their thermal properties are compared with those of related homopolymers.

DISCUSSION

Polymer Structure. The gCOSY, HSQC, HMBC, ^{13}C NMR, and ^{1}H NMR analysis of the copolymers and comparison with spectra of PEA and PIB homopolymers provide evidence for the presence of the copolymer segments shown in Chart 1. The connection of IB to EA units via b−A and b−A′ follows from 2D NMR as shown in Chart 2. Correlations between different groups located within the copolymer that were identified using 2D NMR methods (Table 2) provide a picture of the local structures but do not provide long-distance information, nor do they differentiate between regularly repeating short blocks and more random copolymer structures.

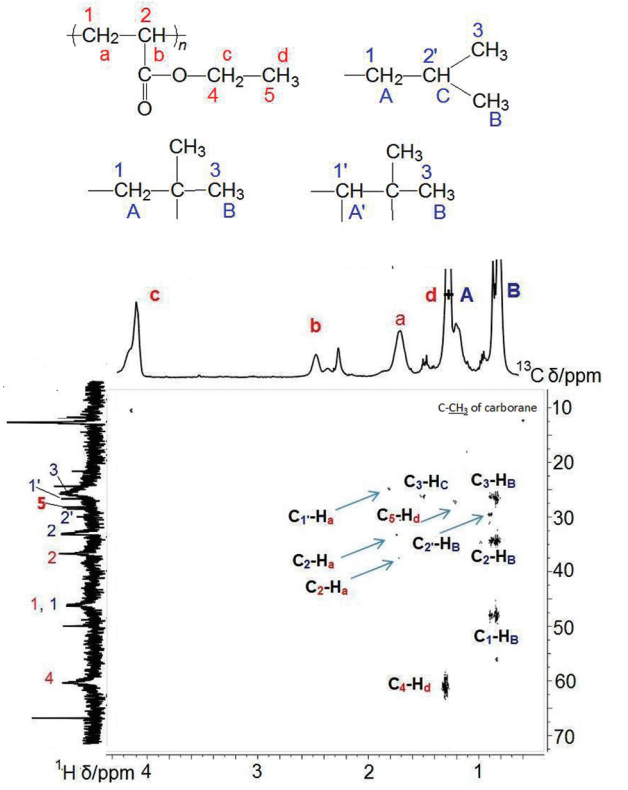

Figure 7. gHMBC NMR spectrum of typical copolymer with proposed assignments.

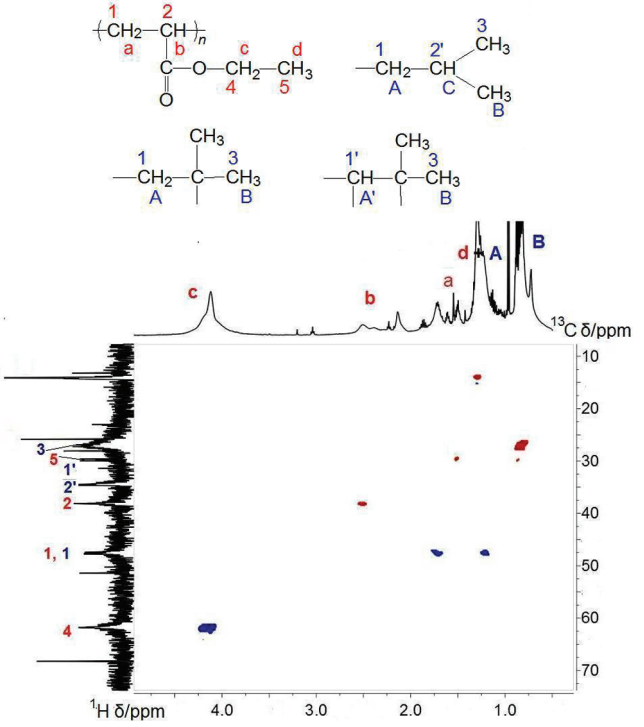

Figure 8. gHSQC NMR spectrum of typical copolymer with proposed assignments. Red: CH_3 and CH groups; blue: CH_2 groups.

dx.doi.org/10.1021/ma101926c |Macromolecules 2011, 44, 2552–2558

Table 2. Summary of 2D NMR Spectra

unit	COSY	gHSQC	gHMBC
EA	c−d, a−b	C_2-H_b, C_4-H_c, C_1-H_a	C_5-H_c, C_4-H_d, C_5-H_d, C_2-H_a
IB	A−C, C−B	C_3-H_B, C_1-H_A, C_1-H_A	C_3-H_C, C_3-H_B, C_2-H_B, $C_{2'}-H_B$, C_1-H_B, C_2-H_A
EA−IB	b−A, a−A		C_2-H_a, C_1-H_a

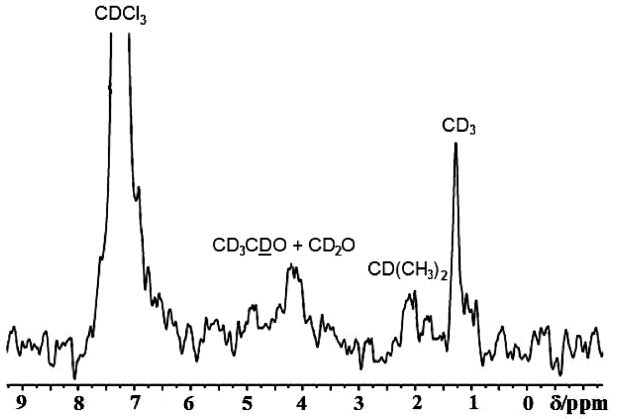

Figure 9. ^{2}H NMR spectrum of copolymer prepared from EA-d_5 and IB (run 9 in Table 1).

Table 3. Glass Transition Temperature (T_g) and Decomposition Temperature (T_d)

polymer	T_g (°C)	T_d (°C)
PEA[26]	−22	337
l-PIB	−40	300
b-PIB	15	221
copolymer	−18 to −10	250 to 430

Chart 1. PIB Segments in the Copolymer

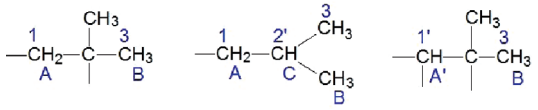

Chart 2. Copolymer IB−EA Linkage Fragments

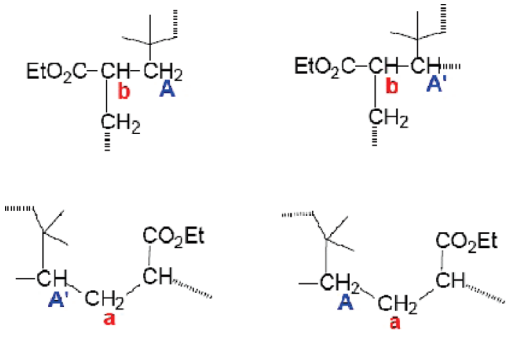

Polymer Composition. HPLC data in comparison with the same data for pure PEA and PIB with different M_w presented in Figure 2 allow us to conclude that our products are copolymers and not a mechanical mixture of two homopolymers, in agreement with the conclusion drawn from the gradient NMR results.

In view of the much higher reactivity of EA in radical polymerization, it is remarkable that the use of a large excess of IB over EA permits an incorporation of IB into the copolymer to an extent as high as ∼56 mol % (Table 1). The extent of IB incorporation depends primarily on the monomer ratio. The dependence may be complicated by the dependence of the aggregation state of the lithium catalyst and thus its reactivity on the detailed composition of the solution.

Polymerization Mechanism. The generally poor behavior of IB in radical polymerization is believed to be due to degradative chain transfer that dominates over propagation.[27] We propose that this dominance is reduced or removed in the presence of Li^+, capable of activating IB toward propagation by complexing to it. The copolymerization pathways proposed to operate in the presence of a large excess of IB are presented in Scheme 1. In the first step, the electron-rich *tert*-butyl radical formed by the decomposition of ATB adds to the electron-deficient double bond of the IB−Li^+ complex or to the similarly electron-deficient double bond of EA, yielding the b−A linkage in the copolymer. In the first case, the addition yields an electron-rich *tert*-alkyl radical similar to the starting *tert*-butyl radical. In the second case, the addition produces an electron-poor radical that is likely to attack a double bond in IB, again producing an electron-rich *tert*-alkyl radical. This will behave similarly as the initial *tert*-butyl radical, adding to the double bond of either the IB−Li^+ complex or the EA comonomer. The repetition of the steps builds up the main chain. After several molecules of either monomer have been incorporated and formed a longer chain, the radical end of the chain can also abstract a hydrogen atom from a methylene group contained in the main chain. This terminates a side chain and transfers the main chain propagation center to a new location.

The unexpected relative peak intensities in Figure 9 and the presence of a peak possibly attributable to $-CD(CH_3)_2$ hint that the IB-based radical end of the chain might also be able to abstract a hydrogen atom from the ester ethyl group of the EA moiety. Such abstraction is unusual in the homopolymerization of EA. Because of the poor signal-to-noise ratio, the ratio of peak intensities in Figure 9 is not sufficiently reliable for a definitive claim. Since such abstraction would place an ester link into the backbone, we looked for substantial degradation of molecular weight upon acidic hydrolysis of the copolymer, but did not find it under conditions that led to the hydrolysis of the ethyl ester groups. It is conceivable that the hydrolysis of the backbone was not observed because it is too slow, but it is more likely that abstraction from the ester ethyl group does not occur to a significant extent, and we did not investigate the matter further.

The proposed steps account for the structure revealed by NMR. Its main distiguishing features are the comparable reactivity of the double bond of the IB−Li^+ complex and of EA that is responsible for the high incorporation of IB into the copolymer

Scheme 1. Proposed Mechanism for the Copolymerization

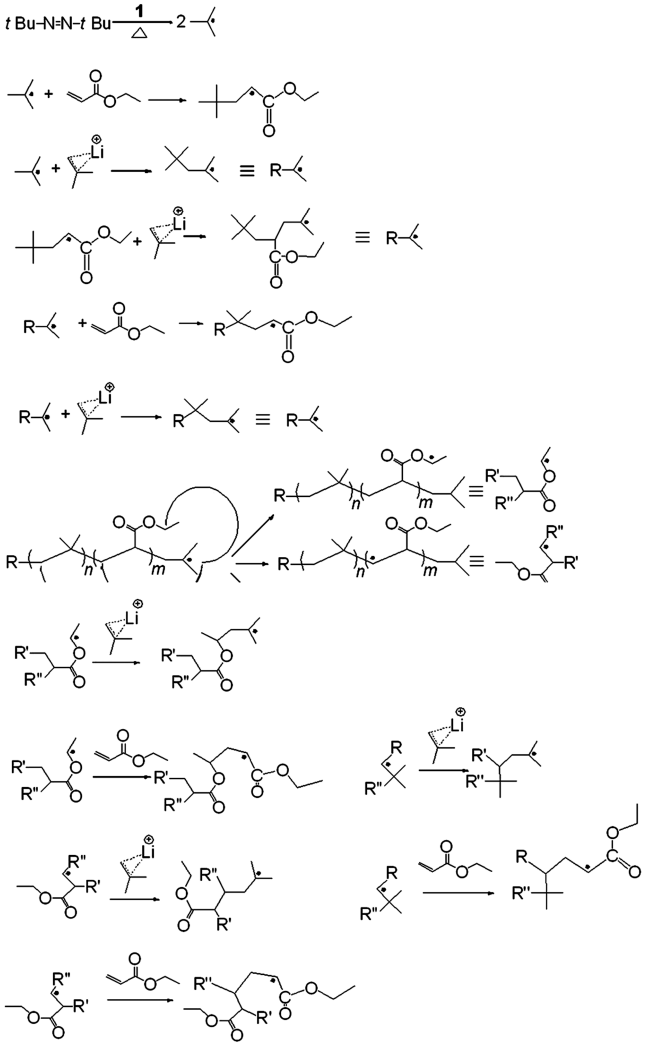

and the propensity for backbiting that is responsible for significant branching. We have NMR evidence for side-chain termination due to abstraction of a hydrogen atom by a *tert*-alkyl radical derived from the insertion of IB. Because of excessive peak overlap, we do not have such evidence for side chain termination by a radical located next to an ester group, derived from the insertion of EA, but it is likely that it occurs as well.

We were pleasantly surprised to find that the presence of the ester group in EA does not inhibit the Li^+-induced catalysis, although it could be expected to bind to Li^+ and deactivate it, as excess sulfolane does. Conceivably, only one ester functionality attaches to Li^+, leaving the cation still able to bind to IB.

Copolymer Properties. Most of the copolymers have higher thermal decomposition temperatures T_d than the homopolymers PEA or PIB (Table 1). All copolymers have higher T_g than that of the PEA homopolymer, but much lower than those of *b*-PIB (Table 3). T_g is closely related to the micro-Brownian rotational motion around carbon−carbon bonds in the polymer backbone. The high T_g of our copolymers may be attributed to the branched IB chain and steric interaction restricting the motion of the polymer backbone,[20] in agreement with the observation in Table 2 that *b*-PIB has a higher T_g than *l*-PIB.

Copolymer M_w increases with increasing incorporation of EA. For copolymers that consist mostly of EA, M_w values up to 1 000 000 were found. Presumably, high incorporation of branched IB changes the conformation of growing polymeric molecules in solution and causes steric difficulties for the approach of the next monomer molecule.

GPC analysis with triple detection shows that the copolymer has a major and a minor component. The major component has a molecular weight distribution similar to those of linear polyolefins produced with Ziegler−Natta catalysts.[28] Relatively low IV value suggests a high density polymer. A Mark−Houwink slope of 0.213 is characteristic of spherical molecules with short branching only (the length of the backbone is longer than the average length of the chains). Also, the almost linear dependence of log R_h on log M_w indicates that the structure of the polymer is much closer to linear than to branched. Small amounts of very high molecular weight polymers, as a minor component of the same fraction, can be indicated by LS and IV, but the RI signal is weak, which is a characteristic of high molecular weight branched polymers such as LDPE.[29] In addition, a lower retention time from LS and UV detectors compared to the RI detector is an indication for a branched polymer.

The origin of the bimodality observed in some cases (Figure 2) is uncertain. It is likely that the state of aggregation of the catalyst and/or its mode or degree of complexation with the ester groups and the IB monomer present are sensitive to minor details of the composition of the solution, and they could change during the polymerization reaction. If they affect the catalytic properties of $LiCB_{11}(CH_3)_{12}$, a bimodal distribution could result easily.

CONCLUSIONS

Somewhat branched copolymers of IB and EA with moderate to high molecular weight and high IB incorporation have been synthesized via radical copolymerization catalyzed by $LiCB_{11}(CH_3)_{12}$. The properties of the copolymers are different from those of the corresponding homopolymers. A copolymerization mechanism has been proposed. The sensitivity of the polymerization process to details of the reaction conditions is attributed to the effects of poorly controlled catalyst aggregation in the relatively nonpolar reaction medium, which requires further investigation.

ASSOCIATED CONTENT

Supporting Information. List of abbreviations and NMR spectra of copolymer from IB-d_8. This material is available free of charge via the Internet at http://pubs.acs.org.

AUTHOR INFORMATION

Corresponding Author

*E-mail: michl@eefus.colorado.edu.

Present Addresses

[‖]Chemistry Department, Xavier University of Louisiana, New Orleans, LA 70125.

[⊥]Department of Natural Sciences, School of Agricultural and Natural Sciences, University of Maryland Eastern Shore, Princess Anne, MD 21853.

■ ACKNOWLEDGMENT

We are grateful to Mr. Matthew T. Holden for assistance, to Dr. Richard K. Shoemaker for help with NMR measurements and interpretation, and to the USARO (W911NF-08-1-0288 and W911NF-09-1-0124) for financial support.

■ REFERENCES

(1) Vyakaranam, K.; Koerbe, S.; Michl, J. *J. Am. Chem. Soc.* **2006**, *128*, 5680.
(2) Volkis, V.; Mei, H.; Shoemaker, R. K.; Michl, J. *J. Am. Chem. Soc.* **2009**, *131*, 3132.
(3) Volkis, V.; Douvris, C.; Michl, J., submitted for publication.
(4) Boffa, L. S.; Novak, B. M. *Chem. Rev.* **2000**, *100*, 1479.
(5) Monakov, I. B.; Zaikov, G. E. *Molecular and High Molecular Chemistry*; Nova Science Publication, Inc.: Hauppauge, NY, 2006; p 269.
(6) Yasuda, H. *J. Organomet. Chem.* **2002**, *647*, 128.
(7) Ouchi, M.; Terashima, T.; Sawamoto, M. *Acc. Chem. Res.* **2008**, *41*, 1120.
(8) Kamigaito, M.; Ando, T.; Sawamoto, M. *Chem. Rev.* **2001**, *101*, 3689.
(9) Braunecker, W. A.; Matyjaszewski, K. *Prog. Polym. Sci.* **2007**, *32*, 93.
(10) Baskaran, D.; Müller, A. H. E. *Prog. Polym. Sci.* **2007**, *32*, 173.
(11) Greenley, R. Z. *Polymer Handbook*, 4th ed.; Brandrup, Immergut Gulke, Eds.; Wiley & Sons: New York, 1999; p 309.
(12) Coca, S.; Coleridge, E. R.; McCollum, G. J.; O'Dwyer, J. B.; Poole, J. E.; Trettel, V. A. WO/2003/070793, 2003.
(13) Brubaker, M. M.; Gleason, A. H. US Pat. 2531196, E. I. duPont de Nemours and Co., 1950.
(14) Sparks, W. J.; Jacobson, R. A. US Pat. 2411599, Standard Oil Development Co., 1946.
(15) Hirooka, M.; Yabuuchi, H.; Kawasumi, S.; Nakaguchi, K. *Polym. Lett.* **1967**, *5*, 47.
(16) Hirooka, M.; Yabuuchi, H.; Kawasumi, S.; Nakaguchi, K. *Polym. Lett.* **1973**, *11*, 1281.
(17) Chen, Y.; Sen, A. *Macromolecules* **2009**, *42*, 3951.
(18) Serniuk, G. E.; Thomas, R. M. US 3183217 Esso Research and Engineering Co., 1965.
(19) Mashita, K.; Kato, T.; Yasui, S.; Hirooka, M. *Polymer* **1995**, *36*, 3949.
(20) Marques, M. M.; Fernandes, S.; Correia, S. G.; Ascenso, J. R.; Caroço, S.; Gomes, P. T.; Mano, J.; Pereira, S.; Nunes, T.; Dias, A. R.; Rausch, M. D.; Chien, J. C. W. *Macromol. Chem. Phys.* **2001**, *201*, 2464.
(21) Fernandes, S.; Marques, M. M.; Correia, S. G.; Mano, J.; Chien, J. C. W. *Macromol. Chem. Phys.* **2001**, *201*, 2566.
(22) Hagman, J. F.; Crary, J. W. In *Encyclopedia of Polymer Science and Engineering*; Mark, H. F., Bikales, N. M., Overberger, C. G., Menges, G., Kroschwitz, J. I., Eds.; Wiley-Interscience: New York, 1985; Vol. 1, p 325.
(23) King, B. T.; Janoušek, Z.; Grűner, B.; Trammell, M.; Noll, B. C.; Michl, J. *J. Am. Chem. Soc.* **1996**, *118*, 3313.
(24) Sebastião, R. C.O.; Pacheco, C. N.; Braga, J. P.; Piló-Veloso, D. *J. Magn. Reson.* **2006**, *182*, 22.
(25) Cheremisinoff, N. P. *Polymer Characterization Laboratory Techniques and Analysis*; Noyes Publications: Wastwood, NJ, 1996; p 8.
(26) Mashita, K.; Hirooka, M. *Polymer* **1995**, *36*, 2983.
(27) Princi, E.; Vicini, S.; Pedemonte, E.; Arrighi, V.; McEwen, I. *J. Appl. Polym. Sci.* **2005**, *98*, 1157.
(28) Mason, A. F.; Coates, G. W. *Macromol. Eng.* **2007**, *1*, 217.
(29) *Handbook of Size Exclusion Chromatography*; Wu, C., Ed.; Marcel Dekker, Inc.: New York, 1995.